

# OPMOS: Ordered Parallel Multi-Objective Shortest-Path

Leo Gold  
University of Connecticut  
Storrs, CT USA  
leo.gold@uconn.edu

Adam Bienkowski  
University of Connecticut  
Storrs, CT USA  
adam.bienkowski@uconn.edu

David Sidoti  
Naval Research Laboratory  
Monterey, CA USA  
david.m.sidoti.civ@us.navy.mil

Krishna Pattipati  
University of Connecticut  
Storrs, CT USA  
krishna.pattipati@uconn.edu

Omer Khan  
University of Connecticut  
Storrs, CT USA  
khan@uconn.edu

## Abstract

The Multi-Objective Shortest-Path (MOS) problem finds a set of Pareto-optimal solutions from a start node to a destination node in a multi-attribute graph. To solve the NP-hard MOS problem, the literature explores heuristic multi-objective A\*-style algorithmic approaches. A generalized MOS algorithm maintains a “frontier” of partial paths at each node and performs ordered processing to ensure that Pareto-optimal paths are generated to reach the goal node. The algorithm becomes computationally intractable as the number of objectives increases due to a rapid increase in the non-dominated paths, and the concomitantly large increase in Pareto-optimal solutions. While prior works have focused on algorithmic methods to reduce the complexity, we tackle this challenge by exploiting parallelism using an algorithm-architecture approach. The key insight is that MOS algorithms rely on the ordered execution of partial paths to maintain high work efficiency. The OPMOS framework, proposed herein, unlocks ordered parallelism and efficiently exploits the concurrent execution of multiple paths in MOS. Experimental evaluation using the NVIDIA GH200 Superchip shows the performance scaling potential of OPMOS on work efficiency and parallelism using a real-world application to ship routing.

## 1 Introduction

In many optimization problems, several distinct (and often competing) objectives need to be optimized. For example, when planning a road trip, one may wish to minimize the driving distance, driving time, and cost of tolls along the route. Similarly, when planning a journey by sea, one may be interested in the fastest and the most fuel-efficient routes, but deciding the right trade-off may depend on the urgency of the matter and the meteorological and oceanographic (METOC) environment.

This paper explores the NP-hard multi-objective shortest-path (MOS) problem, a generalization of the well-known (and polynomial) single-source shortest-path problem [28]. Given a weighted graph with non-negative edge weights, the shortest path problem computes the minimum-cost path

from a start node to a goal/destination node in the graph [33]. In a multi-objective setting, each edge is given a non-negative cost vector (constant length for each edge in a graph), with each element corresponding to an objective. When these objectives compete, generally no single path can optimize all the objectives simultaneously. MOS aims to find a set of Pareto-optimal (non-dominated) solution paths, where a path is Pareto-optimal if no single objective of the path can be improved without causing at least one of the other objectives to deteriorate in quality. For example, (5,4) and (4,5) can be Pareto-optimal path costs to a node. During execution, the intermediate path cost vectors form the so-called *Pareto-optimal labels*<sup>1</sup> that comprise potential candidate solutions. However, computing this front is computationally hard [2, 5, 20, 28], even for two objectives [7]. As the number of objectives increases, so does the computational complexity and the number of Pareto-optimal solution paths [25].

To efficiently compute an exact or approximated Pareto-optimal front, algorithmic solutions are developed based on the multi-objective extension of the A\* algorithm, originally designed for the single-objective search [15, 32, 35]. Multi-objective A\* (MOA\*), unlike A\* which exits once the first solution is found, needs to store a set of Pareto-optimal solution paths to the goal node. MOA\* maintains a priority queue with lexicographical ordering of candidate paths (or labels) to guarantee that only the globally Pareto-optimal paths to nodes are processed. It terminates once the queue is empty. A New Approach to Multi-Objective A\* (NAMOA\*) [15] uses consistent heuristics to improve over MOA\*, and handles an arbitrary number of objectives [25, 26].

In a single-objective shortest path, there can be only one minimum solution path cost for each node in the graph. As seen in Figure 1(a), this is computed using a singular cost comparison for a given node in the graph. However, MOS does not have a single solution path guarantee since multiple non-dominated paths can exist from the start node to any other node in the graph. If a label  $l(v)$  is defined to be a path cost from the source node to a node  $v$ , when a new

<sup>1</sup>MOS literature also identifies a candidate path as a label [16, 25, 27].

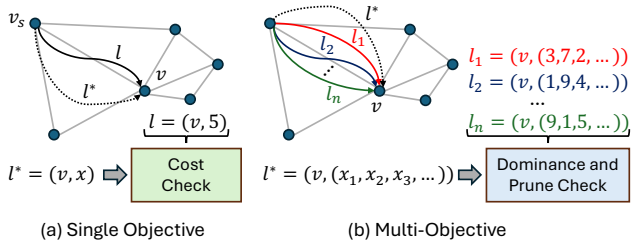


**Figure 1.** Comparison of (a) single objective vs. (b) multi-objective intermediate labels between the source node  $v_s$  and an intermediate node  $v$ . A new candidate label  $l^*$  is shown alongside the associated label-level operations.

candidate label  $l^*(v)$  is discovered, a *dominance check* must be performed to verify if the accumulated cost vector for any previous labels for that node  $v$  dominates the cost vector for  $l^*(v)$ . The label  $l^*(v)$  must be compared with all previously found non-dominated labels to  $v$ , as illustrated in Figure 1(b). If it is not dominated, then the mutually non-dominated set of labels at  $v$  must be updated with the new label, possibly *pruning* existing solutions if the new label dominates them. These dominance and pruning checks are expensive, especially as the number of non-dominated labels increases with the number of objectives. A recent survey paper [26] suggests key challenges facing MOS algorithms. These include tackling the computational complexity of label processing with increasing objectives, choosing the best lexicographic order when ordering the candidate labels, creating scalable and efficient parallel MOS implementations, and generating real-world representative benchmarks for MOS.

Identifying the right labels for parallelization is crucial to unlocking parallel performance potential in MOS. In the sequential setting, a lexicographically ordered priority queue is used to ensure that a globally optimal label is extracted at each iteration [15]. However, when multiple labels are extracted in a parallel setting, the resulting labels may not be Pareto-optimal. Sanders and Mandow [27] come to the same conclusion in their theoretical parallel model for one of the original bi-criteria MOS algorithms [16]. The approach focuses on extracting the global Pareto front at each iteration using a specialized Pareto-queue data structure confined to only two objectives. Sanders and Mandow assert that an exact implementation of the global Pareto queue is unknown for more than two objectives, and suggest a controlled relaxation of label ordering for more than two objectives. This forms the basis for our proposed hypothesis: the work efficiency of MOS needs to be kept in check by extracting labels as close to global Pareto-optimal ordering as possible. With increasing objectives, the priority queue presents more labels that may be close to being globally Pareto-optimal. If high-priority labels are extracted, there exists the potential for a lower reduction in work efficiency since each wasted label

processed is a complex operation with a high order of dominance and pruning checks. The key idea of *ordered queue extraction* is proposed for parallel MOS. It encompasses two main components: candidate label ordering, and the number of labels extracted at each iteration.

We make the following observations from a performance characterization of the MOS framework: (1) the complexity of the algorithm grows substantially with the number of objectives, (2) there is significant room for parallelism given the large time spent in candidate label computations relative to the priority queue operations, and (3) the ordering of the candidate labels is salient for work efficiency. Herein, an Ordered Parallel MOS framework (OPMOS) is proposed to capture the importance of maintaining order in computations while extracting parallel performance for MOS acceleration. It aims to keep the order intact for extracting high-priority labels from a lexicographically-ordered priority queue (PQ) of intermediate non-dominated labels. These labels are distributed among the cores of a multicore processor at each iteration. OPMOS faces load balancing and sequential extractions and updates to the PQ as key performance scaling challenges. The work done for each label is not uniform since intermediate graph connections are explored in an unstructured manner, and each label performs a non-deterministic number of dominance and pruning checks. The challenge worsens as the graph size and the number of objectives increase. A novel label complexity-aware load balancing algorithm is proposed to reduce the load imbalance in OPMOS. When multiple labels are processed in parallel, the updates for the PQ may result in duplicates and new candidate labels that dominate each other. This leads to redundant updates that must be serially applied to the PQ. A novel parallel update reduction method is proposed to reduce the update volume before applying them to the PQ at the end of each iteration. Thus, higher parallelism is unlocked by lowering the impact of expensive serialization update operations. The OPMOS framework allows for parallel execution of MOS for an arbitrary number of objectives. The complexity of PQ extractions increases with the number of objectives. To overcome the serialization latency of PQ extractions, a novel asynchronous execution of parallel label processing is proposed that trades off ordered parallelism and work-efficient execution.

A key challenge in systematically evaluating MOS algorithms is the lack of multi-objective graph benchmarks using real-world applications [26]. Prior works use synthetic graphs to constrain the search space, or use a road network with only two or three objectives [25]. The search space for MOS in the New York City map (264K nodes and 733K edges) is so massive that limited evaluation is performed in [25] by comparing partial solution paths obtained within a runtime limit of 600 seconds. The Tool for Multi-objective Planning and Asset Routing (TMPLAR) [17, 31, 42] is the only framework (to the best of our knowledge) that evaluates real-world maritime ship routing to completion using

MOS algorithms. It uses a spatio-temporal setting and a set of state-space reduction techniques to generate graphs with over 10 objectives using a variety of dynamic weather and ship datasets, presenting real-world scenarios requiring multi-objective path planning. TMPLAR uses the NAMOA\* MOS algorithm to produce ship routes based on an arbitrary number of input objectives. Despite the state-space reduction, many routes are still intractable for high numbers of objectives. Therefore, the maximum number of objectives that complete within a predetermined runtime limit are used to evaluate the proposed OPMOS framework.

This paper makes the following contributions:

- TMPLAR is proposed as a new benchmark for evaluating MOS algorithms due to its ability to process a large number (>10) of objectives and real-world scenarios.
- The MOS framework performance characterization using the NVIDIA GH200 Superchip [19] reveals three core observations about MOS algorithms: the growth in complexity with an increase in objective count, the potential for parallelism due to long computational critical paths, and the importance of ordering the candidate labels for work-efficient parallel execution.
- An OPMOS framework is proposed for parallel MOS execution that is capable of handling an arbitrary number of objectives. OPMOS is applied to TMPLAR and evaluated to highlight the work efficiency and parallelism trade-offs. The evaluation using the 72-core Arm CPU in the GH200 Superchip shows a geometric mean 14× speedup over sequential for the evaluated graphs using NAMOA\*-based MOS algorithms.

## 2 Related Work

The MOS problem is well-studied from an algorithmic perspective, and it is known that generating an exact Pareto front is NP-hard [28]. Alternative genetic and evolutionary algorithms [1, 13, 40, 44] have been explored in the literature but they suffer from computational inefficiencies and poor explainability of the quality of their solutions. Therefore, researchers have focused mostly on tackling the algorithmic complexity of the generative Pareto front approaches as summarized in a recent survey paper [26]. Algorithmic techniques have been explored to reduce the runtime complexity or approximate the Pareto front using label-setting or label-correcting approaches. Martin’s algorithm [16] is a label-setting algorithm that extends single-objective Dijkstra to the multi-objective setting. MOA\* [32] introduces A\* to the multi-objective domain. Since then many improvements over MOA\* have been explored in the literature, with NAMOA\* [15] serving as the basis of most modern advancements [26]. The algorithmic enhancements include: dimensionality reduction (NAMOA\*-dr [24]), lazy versus eager dominance checks (BOA\* [35]), and enhanced data structures (EMOA\* [25]), among others [26].

While these algorithmic optimizations have been proposed, most focus on two or three objectives due to the exploding size of the search space induced by the larger number of objectives [25, 26]. NAMOA\* remains one of the only modern MOS algorithms that applies to an arbitrary number of objectives, establishing itself as the baseline for this paper. However, the proposed ordered parallel model applies to other MOS algorithms as we will explore in future work. Due to the NP-hard nature of the exact generative algorithms, approximations to the Pareto front have also been explored to lower the complexity at higher objective counts through runtime state-space reductions. Warburton [39] introduces an  $\epsilon$ -based procedure that allows approximate dominance checks to enable pruning of paths within an  $\epsilon$ -bounded range. Several optimizations to the approximation strategy have been introduced [2, 3, 10, 34]. The quality of solutions is impacted with approximations, introducing a trade-off between runtime efficiency and solution quality [42]. However, the  $\epsilon$ -optimal approximation enables the NAMOA\* to push the limits on the number of objectives.

So far, all discussed strategies tackle the MOS complexity from an algorithmic perspective. Parallel MOS is an under-explored method of handling the complexity as the number of objectives increases [26]. Sanders and Mandow [27] present a parallel variant of Martin’s algorithm in the bi-objective setting. It constructs a true Pareto queue to allow parallel extraction of all globally Pareto-optimal labels at each iteration, which the authors assert is not practical for more than two objectives. Focusing on theoretical analysis, this paper does not introduce an implementation or experiments and notes that the proposed algorithm may not be practical. Others attempt parallelization by launching multiple MOS instances with different lexicographical orderings of objectives [26]. However, there is no known single-instance parallel MOS model in the literature capable of handling an arbitrary number of objectives. In this paper, we aim to address the complexity problem for higher numbers of objectives using ordered parallelism.

Ordered graph processing is the cornerstone of extracting parallelism in modern graph applications [9, 21]. Various concurrent priority schedulers for graph analytics have been introduced in the literature, ranging from hardware-centric to software approaches. Swarm [14] and its variant Hive [22] propose speculative execution of tasks in hardware to achieve super-linear speedups for task parallel graph problems, such as single-source shortest paths (SSSP). HD-CPS [29] proposes a hardware-software co-design to trade off work efficiency and parallelism in concurrent priority schedulers for task parallel graph processing. Many CPU and GPU frameworks have also been proposed for ordered graph processing, such as MBQ [41], Galois [18], GraphIt [43], and Gunrock [38]. Recently, researchers have explored specialized approaches for hard-to-scale graph problems (like SSSP) using GPU architecture-specific optimizations [37]. While all these

ordered graph frameworks and enhancements show promise, no work has pursued these methods for the MOS problem. Our proposed approach to exploiting ordered parallelism in MOS can fit into any ordered graph processing framework. However, we propose a general-purpose ordered parallelization of the MOS problems in this paper. We introduce a baseline sequential MOS execution model, then describe the proposed ordered parallel model and use a real-world use case of multi-objective path planning with application to ship routing using the TMPLAR framework [17, 31, 42] for performance evaluation.

### 3 Background and Complexity of MOS

Consider an input graph  $G = (V, E, c)$  with a set of nodes  $V$ , edges  $E$ , where each edge has a set of cost values in  $c$  with  $d$  objectives. For each edge  $e \in E$ , there is a non-negative cost vector  $c(e)$  of length  $d$ . Given a source node  $v_s$  and a goal node  $v_g$  in the graph  $G$ , the path from  $v_s$  to an intermediate node  $v_i$  is defined as  $\pi(v_i)$ , represented by a sequence of nodes where each node is connected to its predecessor on the path. For each path  $\pi(v_i)$ ,  $\hat{g}(\pi(v_i))$  denotes the path cost from  $v_s$  to  $v_i$ , calculated as the sum of the cost vectors  $c(e)$  for all edges present on the path. Since multiple objectives may compete, MOS introduces a dominance check such that given two paths  $a = \pi_1(u)$ ,  $b = \pi_2(u)$  with  $d$  objectives,  $a$  dominates  $b$  (denoted  $a \succeq b$ ) if and only if  $\hat{g}(a)[i] \leq \hat{g}(b)[i]$ ,  $\forall i \in 1, 2, \dots, d$ , and  $\hat{g}(a)[i] < \hat{g}(b)[i]$ ,  $\exists i \in 1, 2, \dots, d$ . All non-dominated paths from  $v_s$  to  $v_g$  constitute the *Pareto-optimal* solution set. MOS aims to find a *cost-unique* Pareto-optimal solution set where no two paths in the subset have the same cost vector.

A few additional terms must be introduced to describe the MOS framework. A label  $l = (v, \hat{g})$  is a tuple containing a node  $v \in V$  and a cost vector  $\hat{g}$ . This represents an intermediate solution path from  $v_s$  to  $v$  with a cost vector  $\hat{g}$ . For simplicity, we denote  $v(l)$  to be the vertex and  $\hat{g}(l)$  to be the cost vector contained in  $l$ . A label  $l$  is dominated by another label  $l'$  if they share the same vertex ( $v(l) = v(l')$ ) and  $\hat{g}(l) \succeq \hat{g}(l')$ . A heuristic vector  $\hat{h}(v)$  is an *admissible* heuristic such that it dominates (less than or equal for all objectives) all Pareto-optimal solutions from node  $v$  to the goal node [15]. A vector  $\hat{F}(l)$  denotes the estimated path cost from the start node to the goal node for a given label, calculated as  $\hat{F}(l) = \hat{g}(l) + \hat{h}(v(l))$ . Let OPEN be a queue of labels prioritized by  $\hat{F}(l)$  in increasing lexicographic order. For each vertex  $u \in V$ , let  $\alpha(u)$  denote the *frontier* set at node  $u$ , holding all non-dominated labels  $l$  at node  $u$ . Each label in  $\alpha(u)$  is a non-dominated partial solution path from  $v_s$  to  $u$ . In NAMOA\*,  $\alpha$  is split into two sets  $G_{OP}$  and  $G_{CL}$ , the open and closed sets, respectively. Here,  $G_{OP}$  contains a per-node set of all partial solution labels in OPEN, while  $G_{CL}$  contains the remaining non-dominated solution labels in the frontier set of each node. Every label in  $\alpha(u)$  can be found in

---

#### Algorithm 1 MOS Framework based on NAMOA\*

---

**Input:** Edge costs  $C$ , heuristics  $H$ , start  $v_s$  and goal  $v_g$  nodes

```

1: OPEN  $\leftarrow$  PriorityQueue( $\emptyset$ );  $P \leftarrow \emptyset$ 
2:  $G_{OP}(u) \leftarrow \emptyset, G_{CL}(u) \leftarrow \emptyset, \forall u \in V$ 
3:  $l_s \leftarrow (v_s, \hat{0})$ 
4: OPEN.insert( $l_s$ ),  $G_{OP}(v_s)$ .insert( $l_s$ )
5: while OPEN  $\neq \emptyset$  do
6:    $l \leftarrow$  OPEN.popmin()
7:    $G_{OP}(v(l)).remove(l)$ ;  $G_{CL}(v(l)).insert(l)$ 
8:   if  $v(l) = v_g$  then
9:     PruneOPEN( $l$ )
10:    Prune $G_{OP}(l)$ 
11:    if NotDominated( $l, P$ ) then
12:       $P.insert(l)$ 
13:   else
14:     for all  $v' \in$  GetNeighbors( $v(l)$ ) do
15:        $l' \leftarrow (v', \hat{g}(l) + \hat{c}(v(l), v'))$ ; parent( $l' \leftarrow l$ )
16:        $\hat{F}(l') \leftarrow \hat{g}(l') + \hat{h}(v(l'))$ 
17:       if not Visited( $v'$ ) then
18:         if NotDominated( $\hat{F}(l'), P$ ) then
19:           OPEN.insert( $l'$ )
20:            $G_{OP}(v(l')).insert(l')$ 
21:         else if Duplicate( $l'$ ) then
22:           continue
23:         else if NotDominated( $l', G_{OP}(v(l'))$ ) and
24:           NotDominated( $l', G_{CL}(v(l'))$ ) then
25:           Prune( $G_{CL}(v(l')), l'$ )
26:           PrunedLabels  $\leftarrow$  Prune( $G_{OP}(v(l')), l'$ )
27:           for all  $l^* \in$  PrunedLabels do OPEN.remove( $l^*$ )
28:           if NotDominated( $\hat{F}(l'), P$ ) then
29:             OPEN.insert( $l'$ )
30:              $G_{OP}(v(l')).insert(l')$ 
31: return  $P$ 
```

---

either  $G_{OP}(u)$  or  $G_{CL}(u)$  for all nodes  $u \in V$ . NAMOA\* also maintains the *Pareto-optimal solution front*,  $P$ , holding the frontier set at the goal node ( $\alpha(v_g)$ ). The output of NAMOA\* creates an *exact* set of Pareto-optimal solution paths in  $P$ .

As shown in Algorithm 1, after initializing the data structures (lines 1-2), a label for the start node  $l_s = (v_s, \hat{0})$  is created and inserted into both OPEN (with priority  $\hat{0}$ ) and  $G_{OP}(v_s)$ . At each iteration (lines 6-30), the label with the lexicographically lowest  $\hat{F}$ -vector is extracted from OPEN. This label  $l$  is removed from  $G_{OP}$  and inserted into  $G_{CL}$  (line 7) to update the frontier sets. At this point, there are a few important procedures to define.

**NotDominated (I, S)** compares  $l$  with labels in a given set  $S$  to verify if a label exists in  $S$  that dominates  $l$ . It returns *false* if  $l$  is dominated by a label in  $S$ , and returns *true* otherwise.

**Prune (S, l)** searches through all labels in a given set  $S$ , and removes all labels  $\in S$  that are dominated by  $l$ .

**PruneOPEN (l)** searches the entire OPEN and removes all labels  $\in$  OPEN that are heuristic-dominated by  $l$  (i.e.  $\hat{F}(l^*) \succeq \hat{F}(l)$  for an  $l^* \in$  OPEN).

**Prune<sub>GOP</sub> (I)** searches through  $G_{OP}(u)$  for all  $u \in V$  and removes all labels that are heuristic-dominated by  $l$  (i.e.  $\hat{F}(l^*) \succeq \hat{F}(l)$  for an  $l^* \in G_{OP}$ ).

If  $l$  is at the goal node ( $v(l) = v_g$ , line 8), *Prune<sub>OPEN</sub>* and *Prune<sub>GOP</sub>* are called (lines 9-10) to prune out any labels dominated by this label. These operators require computationally expensive full index searches through *OPEN* and *GOP* every time the goal node is reached. Due to the rapid increase in the candidate labels with the increasing number of objectives, the complexity of these operators grows substantially with the number of objectives. Then, *NotDominated* is called to check if  $l$  is not dominated by any labels in  $P$  (line 11), and if successful  $l$  is inserted into the Pareto-optimal solution front  $P$  (line 12). The complexity of this operation is proportional to the number of candidate labels in  $P$ , which grows with the increasing number of objectives.

If  $l$  is *not* at the goal node, then all neighbors  $v'$  of  $v(l)$  are explored (line 14). For each  $v'$ , a new candidate label  $l' = (v', \hat{g}(l) + \hat{c}(v(l), v'))$  is generated by extending  $l$  from  $v(l)$  to  $v'$ . The parent pointer of  $l'$  is set to  $l$  to allow solution path reconstruction once execution concludes (line 15). The new  $\hat{F}(l')$  is also computed, combining the new path cost  $\hat{g}(l')$  with the heuristic cost  $\hat{h}(v(l'))$  (line 16) to create a lower-bound estimate of the total path cost from the source  $v_s$  to the goal node  $v_g$ . If  $v'$  is explored for the first time (line 17), then extra computations can be skipped under the assumption that  $G_{OP}(v')$  and  $G_{CL}(v')$  are empty. Before  $l'$  can be inserted into *OPEN* and *GOP* (lines 19-20), *NotDominated* is called (line 18) to check if the lower-bound path estimate ( $\hat{F}(l')$ ) is dominated by any goal-node solutions in  $P$ . The complexity of this operator is also proportional to candidate labels in  $P$ .

If  $v'$  has been visited, then  $l'$  is compared against the labels in  $G_{OP}(v(l'))$  and  $G_{CL}(v(l'))$  in procedure *Duplicate(l')* to check if  $l'$  is a duplicate label, and if it is, the rest of the iteration is skipped (lines 21-22). Otherwise, dominance checks are performed to see if any label in  $G_{OP}(v(l'))$  or  $G_{CL}(v(l'))$  dominates  $l'$  (lines 23-24). The complexity of the duplicate and dominance checks depends on the number of candidate labels in  $G_{OP}$  and  $G_{CL}$  for this node, which grows with the number of objectives. If  $l'$  is not dominated, all labels from the frontier set of  $v(l')$  dominated by  $l'$  are pruned (lines 25-26). The labels pruned from  $G_{OP}$  are memorized to prune them from *OPEN* and avoid full index search (line 27). Before  $l'$  can be inserted into *OPEN* and *GOP* (lines 29-30), *NotDominated* is called (line 28) to check if the lower-bound path estimate ( $\hat{F}(l')$ ) is dominated by any goal-node solutions in  $P$ . Again, the complexity of the dominance check operator is proportional to candidate labels in the set searched ( $P$ ,  $G_{OP}$  and  $G_{CL}$  for this node). The *Prune* operators' complexity also increases with candidate labels being processed for a given node, which grows with the number of objectives.

Once *OPEN* is empty, the algorithm terminates and  $P$  contains the final labels representing the Pareto-optimal solution

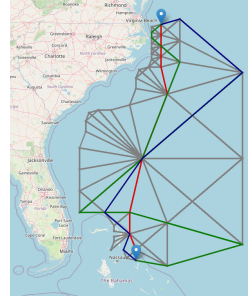


**Figure 2.** Default TMPLAR route from Roanoke Island, North Carolina to Rock Sound, The Bahamas used in [42]. This is labeled as Route 1 in Table 2, Section 6. A subset of Pareto-Optimal Solution Paths are highlighted in color over the state-space reduced graph.

paths (also referred to as exact solutions). Each label processed during the MOS execution performs unstructured and nondeterministic work. Depending on the graph characteristics, each label processed may explore an arbitrary number of adjacent labels. For each neighbor label, a nondeterministic number of labels must be compared via dominance and pruning checks. As discussed earlier, the complexity of these operators relies on the number of candidate labels being compared against, which grows with increasing objective count. Given the high complexity of each label processed, NAMOA\* emphasizes reducing the work being performed. *OPEN* is implemented using a Priority Queue with lexicographical ordering of objectives, guaranteeing a global Pareto-optimal label is extracted at each iteration. This ensures a candidate label with the highest chance of remaining in the final solution is processed, reducing redundant work.

## 4 Characterization and Motivation

There are no standard benchmarks for evaluating multi-objective shortest-path and search algorithms, thus making it difficult to characterize computational challenges and compare results [26]. Many representative graph datasets, such as road networks, are too big for MOS to handle due to the rapid explosion of the state space with increasing numbers of objectives [25]. TMPLAR attempts to solve this challenge through the use of a variety of graph state-space reduction techniques [31, 42]. A forward and backward single-source shortest path (SSSP) is performed to compute a bounding box of reachable nodes to reduce the search space while also creating a time expansion of the graph to account for weather conditions over time. Then, an *admissible* heuristic for NAMOA\* is evaluated using SSSP for each objective and populates the edge weights. Using these techniques, TMPLAR generates directed spatio-temporal graphs with >10 objectives for the maritime ship routing application. The details about the routes (Table 2) and objectives (Table 1) are discussed in the methodology Section 6. However, to characterize the computation challenges, the NAMOA\* algorithm is evaluated for the sequential MOS Algorithm 1 using the representative TMPLAR route shown in Figure 2.

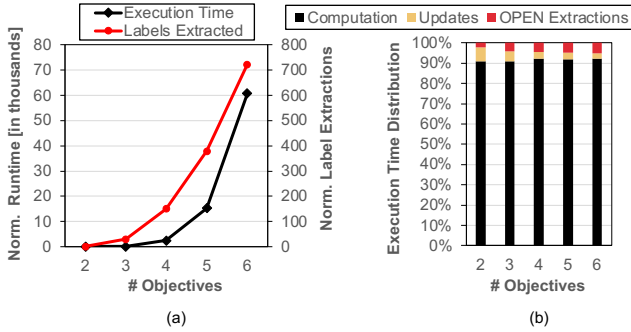


**Figure 3.** TMPLAR Route 1 sequential MOS characterization for two to six objectives. (a) shows relative runtime performance and labels extracted both relative to two objectives, and (b) shows the distribution of execution time breakdowns.

Figure 3a shows the measured execution time and the number of labels extracted (popped) from OPEN with increasing objective count. The OPEN extractions are established as a metric of work efficiency, giving insight into the amount of work performed and the algorithmic complexity. As the number of objectives increases, the execution time increases rapidly, as does the relative work inefficiency (labels popped). The execution time of 0.2 seconds is recorded for two objectives, which rises dramatically to nearly 3.5 hours for six objectives. Beyond six objectives, the optimal setting is intractable, hitting an imposed 16-hour simulation time limit. This shows quantitatively the growth in complexity, measured in both runtime and labels popped, and the clear correlation between these metrics.

For more insights, the execution time is split into candidate label computations (dominance checks, pruning checks, and cost/heuristic computations), updates in OPEN,  $G_{OP}$  and  $G_{CL}$ , and OPEN extractions. Figure 3b shows the runtime breakdown for the 2 to 6 objective sweep. The majority of time is spent on computations, not updates or priority queue (OPEN) operations. The updates for each label can be performed in bulk before extracting a new label from OPEN, decoupling the extraction/updates from the label computations. If multiple labels can be processed simultaneously, these independent computations can be performed in parallel and improve the runtime efficiency of the MOS framework.

A key factor for processing labels in parallel is extracting multiple labels in a given iteration. A single global Pareto-optimal extraction per iteration is used as a baseline for work efficiency. If the OPEN priority queue is maintained, the top  $n$  labels can be extracted, keeping the global order intact but without guarantee that labels after the first extraction are globally Pareto-optimal. Figure 4a shows the relative decrease in work efficiency for this implementation as the number of labels popped increases at each iteration. The results show that as the number of objectives increases, this basic multi-pop strategy extracts more global Pareto-Optimal

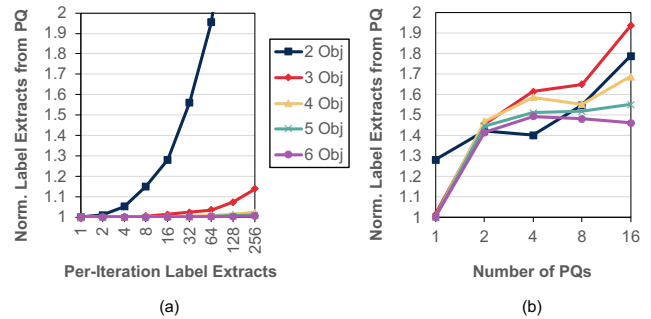


**Figure 4.** TMPLAR Route 7 sweep of (a) label extractions from a single priority queue (PQ), and (b) multiple PQs using a fixed (16) number of labels popped per iteration. Total label extractions normalized to one PQ and extract per iteration.

solutions, thereby reducing the impact on work inefficiency. This allows more labels to be extracted in parallel at higher objective counts without significantly impacting work efficiency.

Ordered processing is a highly explored area in the literature on graph processing. One key issue is the extraction of multiple high-priority labels. MOS is unique given that it performs significant work for each label, making it very sensitive to work efficiency. In general, graph algorithms have only a few (tens) instructions per node to process, where extra iterations are acceptable when they come with the potential for higher orders of parallelism. In MOS, the work for each label is significant, therefore wasted label computations have a considerable impact on performance (see Figure 3, where execution time scales two orders of magnitude higher than the number of labels extracted). Multiple priority queues are explored for concurrent high-priority label extraction to trade off parallelism and work efficiency for ordered graph processing [23, 29, 41]. The nodes in the graph are chunked into buckets, with each bucket getting a priority queue. This improves concurrency in accessing the priority queue but adversely affects priority among candidate labels. To quantify this trade-off, a multi-priority queue is evaluated for the MOS framework. For characterization, the number of labels popped at each iteration is fixed to 16, with the multiple priority queues extracted in a round-robin fashion at each iteration. Therefore, the single priority-queue implementation is the same as the 16-label case in Figure 4a. The results in Figure 4b show the work efficiency of a sweep of priority queues measured by the total number of label extractions relative to the baseline sequential work efficiency established in Figure 3. Little impact is observed at a single priority queue, but work efficiency worsens with multiple priority queues. The general trend is that multiple priority queues result in extractions farther from the global Pareto front, indicating the importance of maintaining the ordering of labels.

---

**Algorithm 2** OPMOS Framework

---

**Input:** Edge costs  $C$ , heuristics  $H$ , start  $v_s$  and goal  $v_g$  nodes

- 1: Initialize Data Structures  $OPEN, GOP, GCL, P, B$
- 2:  $OPEN\_INS, OPEN\_DEL, GCL\_DEL, P\_INS$  in ShMem
- 3:  $l_s \leftarrow (v_s, \hat{0})$
- 4:  $B.insert(l_s), GCL(v_s).insert(l_s)$
- 5: **while**  $B.length() > 0$  **do**
- 6:   GoalNodePhase1  $\leftarrow false$
- 7:   **Phase 1: Label Distribution**
- 8:   **if**  $B.isGoalNode$  **then**
- 9:     GoalNodePhase1  $\leftarrow true$
- 10:    GoalNodeDistribute( $B.removeLast()$ , workers)
- 11:    **Parallel** ProcessGoalNode()
- 12:   **else**
- 13:     LoadDistribute( $B$ , workers)
- 14:     **Parallel** ProcessLabel()
  
- 15:   **Phase 2: Asynchronous Label Extraction**
- 16:    $B.isGoalNode \leftarrow false$
- 17:   **while**  $B.length() < num\_to\_pop$  **and**  $OPEN \neq \emptyset$  **do**
- 18:      $l = OPEN.popmin()$
- 19:      $GOP(v(l)).remove(l); GCL(v(l)).insert(l)$
- 20:      $B.insert(l)$
- 21:     **if**  $v(l) = v_g$  **then**
- 22:        $B.isGoalNode \leftarrow true$
- 23:       **break**
  
- 24:   **Phase 3: Label Updates**
- 25:   **if** GoalNodePhase1 **then**
- 26:     GoalNode NonBlockingBarrier
- 27:     ApplyUpdates( $OPEN\_DEL, P\_INS$ )
- 28:   **else**
- 29:     Label NonBlockingBarrier
- 30:     **Parallel** DominanceCheck( $OPEN\_INS$ )
- 31:     **Parallel** DuplicateCheck( $OPEN\_DEL, GCL\_DEL$ )
- 32:     Label NonBlockingBarrier
- 33:     ApplyUpdates( $OPEN\_INS, OPEN\_DEL, GCL\_DEL$ )
- 34: **return**  $P$

---

Three key observations are highlighted from sequential MOS characterization: the complexity grows with the number of objectives, there is room for parallelism due to the time spent in independent label computation, and a global lexicographical ordering of labels is important to maintaining high work efficiency. This motivates our solution to the MOS complexity problem: multiple labels must be extracted with priority order at each iteration through a single priority queue to exploit parallelism with high work efficiency.

## 5 OPMOS Framework

Ordered Parallel Multi-Objective Shortest-Path (OPMOS) builds upon the MOS framework in Alg. 1, introducing parallel computations in a load-balanced manner while maintaining as close to the global priority of label extractions as possible. At a high level, the main worker extracts a set

of labels from a queue of prioritized labels in lexicographic order (OPEN) and distributes them among workers for parallel execution using a MOS-centric load-balancing scheduler. The extraction and parallel execution of labels is done asynchronously to hide the latency of serial label extractions from OPEN. The individual workers perform the relevant dominance and pruning checks and create updates for the frontier sets and OPEN. The label-centric parallel approach leads to the possible creation of duplicate label updates and labels that may dominate others during the concurrent execution of workers. Since the label updates are performed serially in the main worker to ensure consistency, the volume of these updates can become a bottleneck. Parallel duplicate and dominance checks are proposed to reduce the update volume in the critical code section.

Algorithm 2 presents the pseudo-code for the proposed OPMOS framework. The data structures in OPMOS remain mostly unchanged from Alg. 1. However,  $OPEN, GOP, GCL,$  and  $P$  are initialized in shared memory for efficient parallel access by workers. Four new data structures,  $OPEN\_INS, OPEN\_DEL, GCL\_DEL,$  and  $P\_INS$  are also initialized in shared memory to allow each worker to track its local updates during parallel execution of labels. These data structures are maintained for each worker so they process their updates independently and enable parallel duplicate and dominance checks among the updates. The *bag* data structure,  $B$  contains the metadata for the set of labels to be processed in parallel workers. The labels are extracted from the priority queue (OPEN) using a user-specified number of labels, set as the *num\_to\_pop* parameter. The work done for each label in  $B$  is not only graph-dependent, its complexity grows with the number of objectives and the associated dominance and pruning checks leading to load imbalance. At each iteration, the high-priority labels in  $B$  execute out-of-order in each worker exploiting the work-efficiency and parallelism trade-off discussed in Section 4. OPMOS uses this insight to explore a novel load-balancing scheduler for efficient label-centric parallel execution.

OPMOS executes in three phases at each iteration, as described in Algorithm 2. In Phase 1, the main worker distributes high-priority labels in  $B$  to workers for parallel processing. Immediately following work distribution, the main worker moves to Phase 2 where labels are extracted from OPEN and stored in  $B$  for the next iteration. This allows decoupled (asynchronous) execution of OPEN extractions and parallel label processing, enabling OPMOS to hide the latency of expensive priority-queue operations. After extracting labels from OPEN, the main worker moves to Phase 3 and waits for parallel workers to return with updates. Once all worker updates are received and processed, the next OPMOS iteration commences. Execution continues until there is no more work to be done. This phased execution of OPMOS is discussed in more detail next.

## 5.1 Phase 1: Label Distribution & Parallel Execution

OPMOS initiates execution by inserting the start node  $l_s = (v_s, \hat{0})$  into the  $B$  bag (lines 3-4). After that  $B$  contains the labels for parallel processing in each iteration, and the algorithm continues as long as the bag has active labels for processing (line 5). Details on how labels are inserted in  $B$  are discussed in the next Section 5.2. A naïve load balancer simply distributes each label or a set of labels in  $B$  among workers for parallel execution. However, labels at the goal node,  $v_g$  may have more complexity than regular labels. The full-index searches in *PruneOPEN* and *PruneG<sub>OP</sub>* (lines 9-10 in Alg. 1) are expensive (cf. Section 3), resulting in a long critical path of computations. If these expensive searches are not handled in parallel and instead performed alongside other labels, it leads to a significant load imbalance. On the other hand, if predominantly goal node labels are processed in iterations and the amount of exploitable parallelism is limited in them, then it is beneficial to distribute these labels alongside other labels. A quantitative comparison against the naïve scheduler is presented in Section 7. However, the proposed OPMOS scheduler assumes goal node labels are expensive and treats them separately from other labels for balanced work distribution among workers.

At the start of Phase 1, if a goal node is present in  $B$  (line 8), then a goal node iteration is kicked off to process that label in a load-balanced manner. The goal node label is first removed from  $B$ , potentially postponing the other labels in  $B$  for processing in the next iteration (line 10). In the *ProcessGoalNode* procedure (line 11), the *PruneOPEN* and *PruneG<sub>OP</sub>* functions and  $P$ -dominance and inserts (lines 9-12 in Alg. 1) are performed in parallel. Since *OPEN* and *G<sub>OP</sub>* store the same labels, only one must be searched and pruned. *G<sub>OP</sub>* is organized on a labels-per-node granularity. This allows load distribution to be performed on *G<sub>OP</sub>* by splitting the nodes in the graph into equal chunks and allowing each worker to compute only the sections of *G<sub>OP</sub>* for its assigned range of nodes. The *node-centric* distribution allows the full-index search to be spread across multiple workers. However, this can suffer from load balancing challenges when there is insufficient parallelism due to few labels in *OPEN/G<sub>OP</sub>* per node or high load imbalance due to a few nodes with a high number of labels. A more advanced scheduler that explores more fine-grained parallelism and load balancing will be explored in future work. After load distribution, the *ProcessGoalNode* stores the relevant updates for each worker in *OPEN\_DEL* and *P\_INS*, and once each worker finishes its work, it synchronizes on a barrier. This execution phase is discussed in Section 5.3.

When  $B$  does not contain a label corresponding to the goal node, all labels are removed and distributed among the parallel workers for execution (lines 12-14). A naïve load balancer distributes each label to a worker. However, there is a variation in the amount of work performed for each

label due to the number of neighbors for each label and the number of other candidates to search for each neighbor (cf. Section 3). This variability in work done per label can result in a significant load imbalance leading to diminished parallel performance. The *LoadDistribute* procedure (line 13) mitigates this imbalance by accumulating the total number of neighbors (i.e., candidate labels that will be generated for each label), and splitting these neighbors into equal chunks of labels to be sent to each worker. To analyze the efficacy of this *neighbor-centric* distribution, OPMOS is compared to OPMOS with the naïve load distribution scheduler in Section 7. It is possible to achieve more fine-grained parallelism by splitting up the work for each check (dominance and pruning) at the node granularity, similar to the goal node labels. However, as seen in Alg. 1 there are many dependencies for each check that must be performed in sequence making exploiting parallelism at this granularity challenging. While this is theoretically possible, we explore *neighbor-centric* parallelism in this paper and leave more fine-grained approaches for future work. After load distribution, the labels are processed in parallel by calling *ProcessLabel* (line 14) in each worker to perform its necessary computations, including dominance and pruning checks (lines 15-30 in Alg. 1). Each worker stores its updates in *OPEN\_INS*, *OPEN\_DEL*, and *G<sub>CL\_DEL</sub>*. Once each worker finishes, it synchronizes on a barrier to wait for the other workers to complete. This behavior is further discussed in Section 5.3.

## 5.2 Phase 2: Asynchronous Label Extraction

Extractions from *OPEN* are increasingly expensive at high numbers of objectives due to the higher complexity in the lexicographic ordering of labels and the higher number of active labels in *OPEN*. To hide the latency, *OPEN* extractions are decoupled from label processing. In Phase 2, at each iteration, labels are sequentially removed from *OPEN* and *G<sub>OP</sub>*, and inserted into *G<sub>CL</sub>* and the bag  $B$  (lines 18-20). If a label corresponding to the goal node,  $v_g$ , is extracted (line 21), then the *isGoalNode* flag in  $B$  is set, and the label extractions are paused until the next iteration. Otherwise, the label extractions are continued until either *num\_to\_pop* labels are inserted in  $B$  or *OPEN* has been emptied.

The main worker operates Phase 2 concurrently with parallel label processing initiated in Phase 1. The decoupled execution allows the latency of *OPEN* extractions to be hidden. However, depending on the workload of a given iteration, there may not be enough time to hide the latency of (expensive) *OPEN* extractions. Additionally, since the extraction of labels and their respective updates are now separated across contiguous iterations, this may lead to work inefficiency due to the relaxation of the order of label processing. A naïve approach to label extraction would be to perform serial extractions at the start of each iteration, and then send the bag of labels to the parallel workers (i.e., swap Phase 1 and Phase 2). To quantify, Section 7 compares the asynchronous



bag execution in OPMOS with the naïve OPEN extraction model. Data structures that exploit concurrency in OPEN can also be introduced to reduce the sequential latency of OPEN extractions. For example, the multi-PQ design described in Section 4 can be explored in future work.

### 5.3 Phase 3: Label Updates

When the main worker reaches Phase 3, it waits on a barrier synchronization for the other workers to finish. Like with Phase 1, the next step is determined by the type of bag being processed (goal node or batch of labels). For a goal node iteration (lines 25-27), once all workers reach the barrier synchronization, the main worker calls the *ApplyUpdates* procedure to apply the updates from *OPEN\_DEL* to both OPEN and *G<sub>OP</sub>* and from *P\_INS* to *P* (line 27). Note that the synchronization barrier on line 26 is non-blocking since the updates created by each worker are for an independent set of nodes, and thus do not conflict. Therefore, the main worker begins applying updates from any worker as soon as it finishes, and overlaps computation and communication overheads.

For regular label iterations, once each worker finishes, it synchronizes on a barrier to wait for the other workers to complete. Candidate labels that dominate each other may be produced in a single iteration due to the parallel execution of workers. Although all redundant updates can be applied, they may result in a high volume of updates, leading to significant communication and serialization overheads. To reduce this bottleneck, OPEN inserts (new candidate labels) are compared with each other to check for dominance. The procedure *DominanceCheck* is called in parallel (line 30), where each worker checks its own *OPEN\_INS* buffer against the other workers, and removes the label updates based on the outcome of the dominance check. This procedure also checks for duplicates and uses a worker-ID arbitration strategy to ensure both duplicates are not destroyed (i.e., at least one remains) by only allowing deletes if the current worker’s ID is less than the other worker ID. For the other update data structures, *OPEN\_DEL*, and *G<sub>CL\_DEL</sub>*, only duplicate checks are performed (using the *DuplicateCheck* procedure on line 31). The synchronization barrier on line 29 is non-blocking since each worker only compares its updates to workers who completed the duplicate and dominance checks. This allows for the parallel overlap of the duplicate and dominance check computations with communication overhead. Additionally, the main worker does not need to participate in the first barrier (line 29), since this synchronization ensures all parallel workers complete their assigned processing of labels. This allows the main worker to hide additional OPEN extractions while the duplicate and dominance checks are performed. Once both procedures are complete, another non-blocking barrier is reached (line 32), allowing the main worker to apply the updates from *OPEN\_INS*, *OPEN\_DEL*, and *G<sub>CL\_DEL</sub>*

to OPEN, *G<sub>OP</sub>*, and *G<sub>CL</sub>* in *ApplyUpdates* (line 33). This synchronization is non-blocking since each worker that reaches this barrier has completed all of its update checks, allowing the main worker to apply them as they are received from the parallel workers.

### 5.4 Challenges for OPMOS Framework

Two key challenges arise in the OPMOS framework. First is the sequential nature of the main worker, which extracts labels from OPEN and performs the iteration updates serially. As the number of workers increases, redundant (duplicate) updates may be introduced, which leads to a high update volume. To solve this challenge, the parallel procedures *DominanceCheck* and *DuplicateCheck* are proposed to reduce the update volume by pruning redundancy update operations. Additionally, an asynchronous OPEN extraction method is employed to hide as much of the sequential latency as possible. The second key challenge is the complexity of computations for each label, which unlike other graph algorithms is non-trivial and varies depending on graph properties and the number of objectives in MOS. To solve this challenge, a novel load-balancing approach is proposed to unlock efficient parallel execution. Next, the efficacy of OPMOS is evaluated to quantify its performance scaling potential.

## 6 Methods

The NVIDIA GH200 [19] Superchip’s CPU is used for evaluation. It integrates 72 Neoverse V2 Armv9 cores operating at 3.1GHz in a single chip. The memory hierarchy supports 64KB L1 instruction and data caches, 1MB private L2 cache per core, a shared 114MB last-level cache, and ~500GB of on-package LPDDR5X unified memory with 512GB/s memory bandwidth. Although the system package includes a Hopper NVIDIA H100 GPU interconnected with the CPU using NVLink, it is not used in this paper.

For characterization, OPMOS is implemented in Python 3.10.13 [36], meshing cleanly with the existing Python-based TEMPLAR system. OPMOS is compared against a sequential optimized NAMOA\* MOS algorithm variant. In both the sequential and parallel OPMOS, the frontier sets *G<sub>OP</sub>*, *G<sub>CL</sub>*, and *P* are implemented using optimized NumPy [8] arrays in shared memory with user-managed dynamic array sizing. OPEN is implemented using a heap-based priority queue, which is only accessible in the main worker. In the parallel setting, the main worker uses shared memory buffers to communicate work distribution and retrieve updates from the other workers. The non-blocking barrier in OPMOS (see Section 5) is also implemented using shared memory. To avoid the serialization enforced by Python’s Global Interpreter Lock (GIL) [4], processes are used instead of threads using Python’s multiprocessing library. This allows each worker to run independently in a core, with performance scaling evaluated by varying the number of workers. Faster

#	Obj.	#	Objective	#	Objective
1	Distance	5	Vert. Acceleration	9	Wave Height
2	Fuel	6	Horiz. Acceleration	10	Wave Period
3	Roll	7	Vert. Bending Moment	11	Rel. Wave Bearing
4	Pitch	8	Vert. Shear Force	12	Random

**Table 1.** TMPLAR Objective List. For a given  $n$  objectives run, the first  $n$  objectives are used for lexicographical ordering

sequential and parallel implementations may be possible using compiled programming languages like C/C++, but such optimizations are left for future work.

The evaluation metrics are collected using instrumented performance counters and Python’s `time()` library function for timing measurements. The total number of label extractions, candidate labels explored, and final Pareto-optimal solutions are collected using performance counters. The end-to-end execution time of OPMOS measures the total runtime of the while loop in Alg. 2 (i.e., the runtime does not include the initialization of the data structures and processes). To further describe where time is spent in execution, the runtime is broken into the following components: time spent in **OPEN extractions**, time spent in **updates**, and time spent in **label processing**. For parallel execution, the label processing time for the worst-case worker is further split into the following three components: time spent in **label processing**, time spent in the **duplicate and dominance checks**, and time spent in **communication overheads**.

### 6.1 TMPLAR MOS Benchmark

TMPLAR generates ship routing graphs with up to twelve objectives (as shown in Table 1). The distance objective measures the distance along a line with constant bearing to the true North (the so-called rhumb line distance). Three weather and oceanic parameters are directly used as objectives: wave height, wave direction (relative to ship bearing), and wave period. These parameters are obtained from the ERA5 dataset [11], analyzed at 3-hour intervals starting January 1, 2016. The oceanographic parameters are also used to generate seven objectives: fuel consumption (based on required propulsion in calm water [12] and due to wave resistance [6]), and six ship dynamic response objectives (calculated using a nonlinear wave-load analysis [30]): roll, pitch, vertical acceleration, horizontal acceleration, vertical bending moment, and vertical shear force. A pseudo-randomly generated objective is calculated using a seed of the latitude, longitude, and time window information at each graph edge. TMPLAR allows any number of objectives to be run for a given route, where the objectives are selected in the order specified in Table 1.

TMPLAR’s state-space reduced graph routes used for evaluation are shown in Table 2. These are generated using start and end locations as inputs, along with the start date of January 1<sup>st</sup>, 2016 for weather data information, minimum and maximum ship speeds of 5 and 30 knots respectively, and

Rt. #	Origin (Long., Lat)	Des (Long., Lat.)	Nodes/Edges	Avg Deg.	Max Obj.	Seq. Time(s)
1	Roanoke Isl., NC 75.0°W, 36.0°N	Bahamas 76.0°W, 25.0°N	471, 4394	18.7	6	12,372
2	Alaska 144.4°W, 58.5°N	San Diego 117.6°W, 32.7°N	1690, 10019	12.4	3	16,744
3	Alaska 144.4°W, 58.5°N	Seattle 125.6°W, 48.4°N	461, 2610	11.3	12	560
4	Guam 114.8°E, 13.4°N	Sasebo 134.1°E, 31.5°N	171, 2367	27.7	12	14,586
5	Strait of Gibraltar 7.5°W, 36.0°N	Norfolk, VA 75.0°W, 36.5°N	778, 7787	20.0	4	51,350

**Table 2.** TMPLAR State-Space Reduced Routes

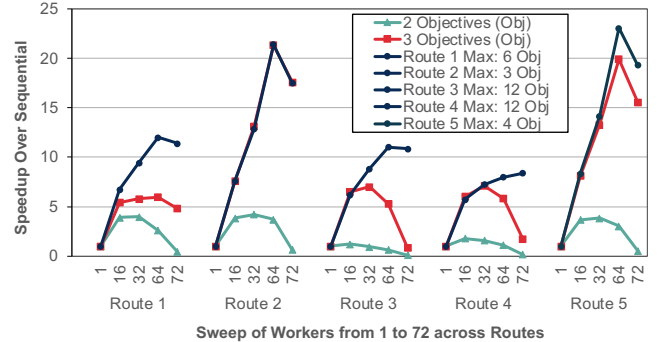


**Figure 5.** OPMOS speedup at increasing workers (and labels) relative to sequential MOS.

a trip length of 14 days ( $\pm 1$  day). Furthermore, the graphs are expanded with 10 time-windows per node to capture temporal weather data variations. The edge weights are populated with data for the user-specified number of objectives. Using these inputs, the graphs in Table 2 are generated for evaluation using the OPMOS framework.

## 7 Evaluation

OPMOS aims to extract parallelism for multi-objective optimization problems. Figure 5 evaluates the performance of OPMOS for two (lowest), three, and the maximum number of objectives achievable for each route (as shown in Table 2). The performance of OPMOS is evaluated by setting the number of label extractions for each iteration (`num_to_pop` parameter) equal to the number of workers and increasing the number of workers from 1 (sequential) to 72. The speedup is shown relative to the sequential MOS framework. For the maximum number of objectives, the performance scales for all routes as the number of workers increases. However, at 72 workers, the number of active processes exceeds the available cores in the CPU, and performance degrades due to scheduling interference by the operating system. The speedups at 64 workers range from  $8\times$  to  $23\times$  with a geometric mean of  $14\times$ . For two objectives, performance scales to a limited number of workers (16-32) and degrades afterward, achieving a geometric mean speedup of only  $2.7\times$ . For Route 3, the performance even falls below sequential at 64 workers. Three objectives observe improved performance speedups

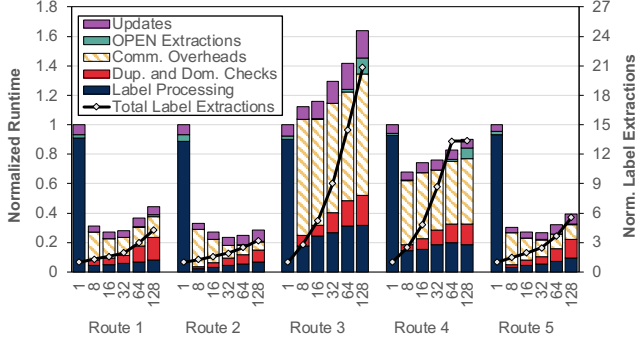


**Figure 6.** Sweep of maximum labels extracted per iteration for 2 objectives using 64 workers.

ranging from  $6\times$  to  $21\times$ , with a geometric mean of  $10.5\times$ . The main reason for lower performance scaling is that work efficiency suffers when multiple label extractions in an iteration result in low-priority labels being processed. The higher the number of objectives, the higher the probability of extracting multiple labels close to the global Pareto front (cf. Section 4). The *num\_to\_pop* parameter relaxes the order in which labels are processed, unlocking parallelism and impacting work efficiency. Other OPMOS optimizations, i.e., asynchronous OPEN extractions, parallel duplicate and dominance checks, and the load balancing scheduler impact work efficiency and parallel performance tradeoffs. These parameters are systematically evaluated for each objective count next, while the number of workers (that are pinned to cores in the CPU) is fixed at 64.

### 7.1 Two Objectives

For two objectives, Figure 6 shows the normalized OPMOS runtime breakdown with per-iteration label extractions swept from 1 to 128. The normalized number of label extractions is also plotted as a metric of work efficiency. At a single extraction per iteration, the optimized sequential MOS is used and the runtime is dominated by label processing. The work inefficiency grows with the number of OPEN extractions but at different rates for each route. Routes 1, 2, and 5 scale to 16-32 workers, and runtime grows with increasing label extractions after that. When work inefficiency is high, more redundant labels are processed, leading to higher label processing times and requiring more duplicate and dominance checks to rectify these inefficiencies. The low-priority labels introduced into the system can also result in more load imbalance and a potential increase in the updates performed. However, the load imbalance (communication overhead component) decreases since more work is exposed to the workers. Routes 3 and 4 observe a massive increase in work inefficiency even when the label extractions are set to 8. Consequently, workers process redundant and wasteful computations that impact all runtime components adversely.

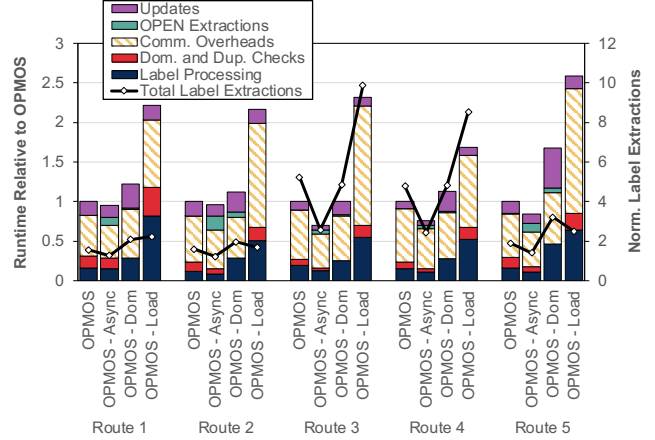


**Figure 7.** Comparisons to OPMOS without asynchronous OPEN extractions (OPMOS-Async), parallel dominance and duplicated checks (OPMOS-Dom), and load-balancing scheduler (OPMOS-Load) for 2 objectives using 64 workers and 16 label extractions per iteration.

Route 3 stands out since it performs worse than sequential even with only 8 label extractions. However, reducing the number of workers improves load imbalance to obtain speedups, as observed for 16 workers in Figure 5.

Figure 7 shows the normalized runtime and the number of label extractions with different optimizations disabled and replaced with the naïve implementations introduced in Section 5. Replacing asynchronous OPEN extractions with sequential label extractions before parallel work distribution (OPMOS-Async) improves performance. This is due to the extreme sensitivity of OPMOS at two objectives to ordered extractions, causing an increase in work inefficiency due to the relaxed order from asynchronous extractions. In route 3, the reduced work inefficiency allows OPMOS-Async to outperform sequential at 64 workers by 18%. This same work efficiency trend is seen across all routes. Removing the duplicate and dominance checks (OPMOS-Dom) shows diminished speedups. Without these checks, the work inefficiency grows causing the updates and label processing times to increase rapidly. The proposed load balancer has the most significant impact on runtime. The naïve approach gives each worker a label regardless of the number of neighbors or if the label corresponds to a goal node. The extreme increase in runtime is attributed to the increasing variability in computational complexity for labels processed. This increases all runtime components with a significant increase in the communication overheads due to worsening load balance.

### 7.2 Three Objectives

For three objectives, Figure 8 shows the normalized OPMOS runtime and label extractions with per-iteration label extractions swept from 1 to 128. The work inefficiency trends

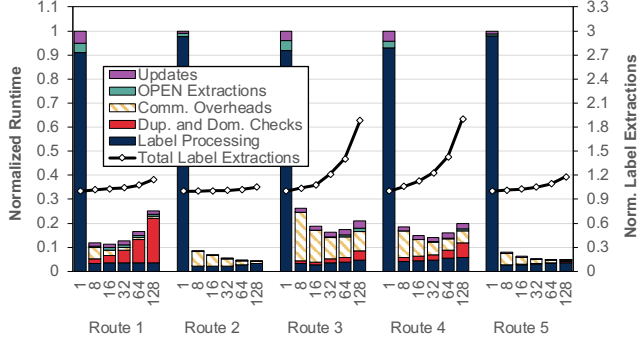


**Figure 8.** Sweep of maximum labels extracted per iteration for 3 objectives using 64 workers.

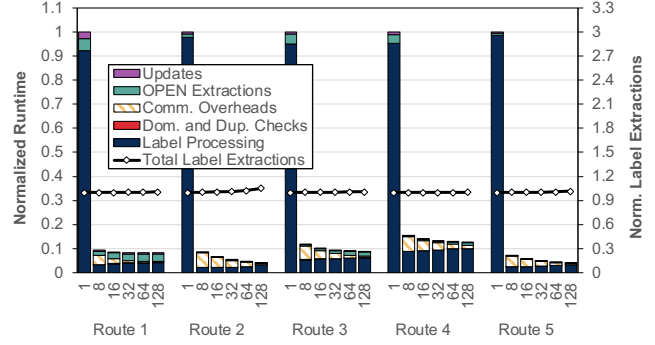


**Figure 10.** Sweep of maximum labels extracted per iteration for maximum objectives (see Table 2) using 64 workers.

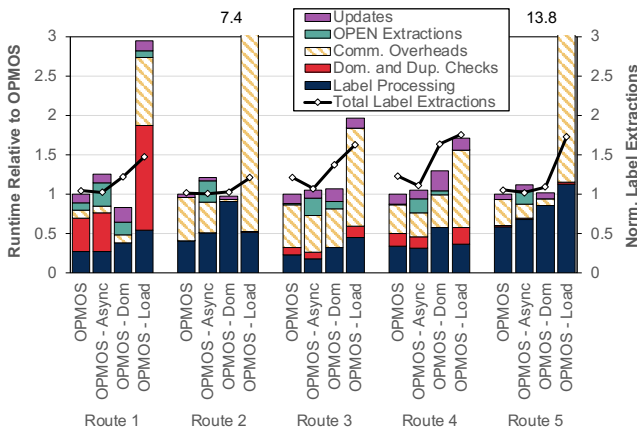


**Figure 9.** Comparisons to OPMOS for OPMOS without asynchronous OPEN extractions (OPMOS-Async), parallel dominance and duplicated checks (OPMOS-Dom) and load-balancing scheduler (OPMOS-Load) for 3 objectives using 64 workers and 32 label extractions per iteration.

continue to increase across all routes but at much-reduced rates. This signifies that with just three objectives many labels close to the global Pareto front are extracted from OPEN. All routes scale to 32 label extractions and routes 2 and 5 up to 128. Even though the increase in work inefficiency causes more label processing times, the communication overheads scale as much of the computations are load-balanced and processed asynchronously. In routes 1, 3, and 4 the update volume and duplicate and dominance checks increase due to low-priority redundant labels, which causes these routes to stop scaling around 32 label extractions.

Figure 9 shows the comparisons to naïve OPMOS optimizations. Unlike the two objectives, the asynchronous OPEN extractions are now more important due to the significant time spent in OPEN extractions. The load balancer keeps the work inefficiency and communication overheads in check, signifying its continued importance. Duplicate and dominance checks are less important at 3 objectives, and can

even be harmful when a high order of costly dominance checks need to be performed, such as in Route 1. While the dominance checks help reduce update volume, they can be expensive if the work done to check for duplicates or dominant labels does not find labels to prune. In this case, the reductions in update volume are unable to overcome the overheads of these checks. In all routes except 1, the dominance check overheads are not a major portion of runtime, and the gains in updates and work efficiency are beneficial. Overall, the work inefficiencies are observed to decrease at three objectives. However, OPEN extractions and duplicate and dominance checks become more costly.

### 7.3 Maximum Number of Objectives

Figure 10 shows the normalized runtime and label extractions for the maximum objectives for each route (as described in Table 2). The trends observed from two to three objectives continue with a lower rate of work inefficiency at increasing label extractions. More time is spent in label processing, OPEN extractions, and communication overheads at these higher objective counts. Updates and duplicate/dominance checks are less of an issue, attributed to the low increase in work inefficiency. The more labels extracted, the more room for further performance scaling. The jump from one (sequential) to 8 label extractions is huge, with a geometric mean speedup of 10×. In all cases, scaling continues up to 128 labels extracted per iteration, with a geometric mean speedup of 14×. These further speedups are obtained mainly by communication overhead reductions, suggesting lower load imbalance with increased parallelism from more labels available for processing. However, OPEN extractions begin to dominate at the higher number of label extractions. Despite this, the results suggest that even higher speedups may be achievable on a CPU with more available cores to exploit parallelism.

Figure 11 shows the comparisons to naïve OPMOS optimizations. Continuing with the trends observed at three objectives, the asynchronous OPEN extractions are dominant since all routes spend a significant portion of runtime

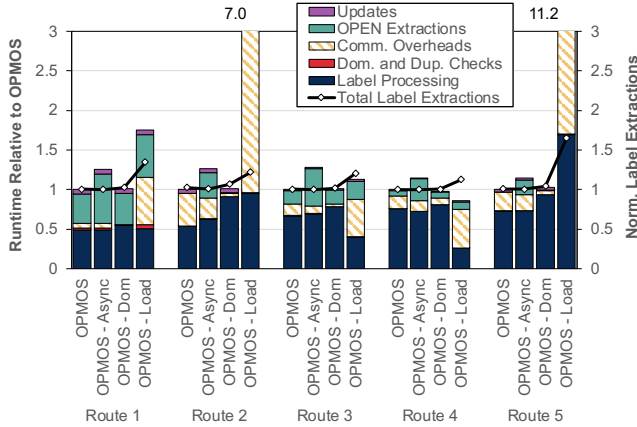


**Figure 11.** Comparisons to OPMOS for OPMOS without asynchronous OPEN extractions (OPMOS-Async), parallel dominance and duplicated checks (OPMOS-Dom) and load-balancing scheduler (OPMOS-Load) for maximum objectives using 64 workers and 64 label extractions per iteration.

on OPEN extractions. Much of the time spent on OPEN extractions can be hidden; only Route 1 with significant OPEN extractions is left with a large chunk of this runtime component in OPMOS. The duplicate and dominance checks barely show up in the runtime, and due to the very low work inefficiency, they have little impact on performance. Due to work efficient execution, a small reduction in update volume is observed, leading to an insignificant effect of duplicate and dominance checks. Load imbalance remains important for exploiting parallelism. Switching to a naïve load balancer results in significantly more time spent in communication overheads, and therefore load imbalance. Routes 3 and 4 see a lower impact on runtime due to load balancing. Route 4 even performs better with a naïve load balancer. This is attributed to increasing goal-node label iterations in these routes (see the last column in Table 3). Since parallelism within a goal-node label may be limited, route 4 benefits from concurrent execution of multiple goal-node labels versus parallelizing a single goal-node label in an iteration. More fine-grained methods for load balancing may be necessary to deal with the load imbalance problem and mitigate the issues with goal node label processing. Overall, it is observed that for high orders of objectives, work inefficiency becomes less of a challenge and OPEN extractions begin to dominate. OPMOS asynchronous OPEN extractions and load-balanced execution overcome these challenges to deliver a geometric mean speedup of 14× over sequential execution.

#### 7.4 Accuracy of Solutions

MOS optimizes all objectives simultaneously and finds a set of Pareto-optimal (non-dominated) solution paths. As the number of objectives increases, so does the number of Pareto-optimal solution paths. The OPMOS framework maintains

Route #	# of Sequential MOS Solutions	OPMOS Match?	% OPMOS Iterations at Goal Node
1	4419	✓	58%
2	3454	✓	21%
3	1432	✓	75%
4	10999	✓	89%
5	10503	✓	57%

**Table 3.** TMPLAR Pareto-Optimal solutions and work-efficiency related metrics for all routes. Correctness is verified by matching all OPMOS output solutions to the sequential MOS solutions.

Route #	Max Obj.	Seq. Time(s)	OPMOS Time(s)	OPMOS Speedup	Seq. #Solns.	OPMOS #Solns.
1	12	64.4	4.1	15.8×	481	321
2	12	84.5	4.8	17.5×	235	204
3	12	4.6	0.26	17.6×	63	44
4	12	13.5	0.98	13.8×	296	208
5	12	86.8	7.5	11.6×	434	381

**Table 4.** TMPLAR using approximate NAMOA\* with  $\epsilon=0.25$

the exact solution sets while extracting maximum parallelism for acceleration. To evaluate the accuracy, the exact solutions are compared to find if the number of solutions and the total cost of each solution match. Table 3 summarizes these results, showing the total number of solutions obtained from sequential MOS, and that for each route at the maximum number of objectives, the solutions match perfectly for OPMOS. This same level of accuracy is observed across all of the routes, objectives, and experiments discussed in this paper.

## 8 Discussion

While each route in TMPLAR can be generated for 12 objectives, not all can execute to completion optimally within the time limit, even within OPMOS. To reduce the complexity of MOS, the approximation parameter  $\epsilon$  has been used to influence the dominance checks [39] to enable pruning of paths within an  $\epsilon$ -bounded range. An  $\epsilon$  of 0.25 allows all 12 objectives to be completed for all evaluated routes, as shown in Table 4. OPMOS is evaluated using  $\epsilon$ -based NAMOA\* and a geometric mean speedup of 15× is observed across all five routes. The gain in performance is not only due to exploitable parallelism but also through a decrease in labels processed relative to the sequential implementation. This is due to the aggressive pruning of candidate labels using the relaxation of the dominance check, thereby preventing similar candidate labels from being introduced. However, this improved performance through parallelism and work-efficiency improvements comes at the cost of solution quality. The number of Pareto-optimal solutions for OPMOS significantly decreases (by as much as 33%) compared to sequential execution with  $\epsilon = 0.25$ . This raises concerns about the explainability of using approximate techniques to reduce the complexity of MOS. Therefore, on the **algorithmic front**, future research must devise methods to understand the relationship between parallelism, work efficiency, and solution quality.

In OPMOS, we explore parallelism at the candidate label level. However, there is significant room for fine-grained parallelism to be explored. Due to computationally intensive labels, individual operators such as *Prune* and *NotDominated* can be parallelized at the granularity of label level checks. Massively parallel single instruction multiple threads (SIMT) architectures are well suited to accelerate dominance and pruning checks. Even novel hardware accelerators can be envisioned to perform these associative lookups efficiently. To unlock parallelism further, an approach that favors parallel execution by disregarding ordered label processing can be implemented where each node in the graph performs dominance and pruning checks in parallel until all nodes settle on a set of Pareto-optimal solutions. This approach will require massively parallel hardware with fast communication to support label-level checks. SIMT architectures, such as modern GPUs, and multi-node high-performance computing (HPC) clusters are candidate architectures that enable such a paradigm. However, on the **architectural front**, future research must devise work-efficient and load-balanced parallel execution to unlock the performance potential of MOS.

Although this paper introduces TMPLAR’s ship routing application as a benchmark for multi-objective shortest paths and search, more research is needed to support routes with increasing graph sizes and diverse applications. MOS can benefit real-world applications, such as road networks, energy grids, autonomous systems, recommendation systems, and social networks, to name a few. Dealing with increasing objective counts requires state space reductions and pre-processing of graph data akin to TMPLAR that generates Pareto-optimal solutions within a time limit. The **benchmarking front** requires future research to create open-source MOS benchmarks for broader community adoption.

## 9 Conclusion

This paper explores the NP-hard multi-objective shortest path (MOS) problem. State-of-the-art MOS algorithms maintain a set of partial paths at each node and perform ordered processing to ensure that Pareto-optimal solution paths are generated. Finding a set of exact solutions becomes computationally intractable as the number of objectives increases. A MOS benchmark capable of handling multiple objectives is proposed for a real-world ship-routing application. It enables state-space graph reduction that enables a tractable execution of MOS for an arbitrary number of objectives. The MOS framework performance characterization using the NVIDIA GH200 Superchip reveals that the computational complexity of MOS grows substantially with the number of objectives. However, due to long computational paths in label processing, there is potential for parallelism. It is concluded that ordered processing of candidate paths is needed for work-efficient parallel execution. Using this insight, the Ordered Parallel MOS (OPMOS) framework is proposed to handle

large numbers of objectives. Novel approaches are proposed to create load-balanced execution while reducing the critical-section operations. The evaluation using 72 Arm cores in the GH200 CPU shows a geometric mean 14× speedup over sequential MOS at the number of objectives as high as 12 using the TMPLAR MOS benchmark generated route graphs.

## References

- [1] Faez Ahmed and Kalyanmoy Deb. Multi-objective path planning using spline representation. In *2011 IEEE International Conference on Robotics and Biomimetics*, pages 1047–1052, 2011.
- [2] Thomas Breugem, Twan Dollevoet, and Wilco van den Heuvel. Analysis of fptases for the multi-objective shortest path problem. *Computers & Operations Research*, 78:44–58, 2017.
- [3] Fritz Bökler and Markus Chimani. *Approximating Multiobjective Shortest Path in Practice*, pages 120–133. 2020.
- [4] Roger Eggen and Maurice Eggen. Thread and process efficiency in python. In *Proceedings of the international conference on parallel and distributed processing techniques and applications (PDPTA)*, pages 32–36. The Steering Committee of The World Congress in Computer Science, Computer ..., 2019.
- [5] Matthias Ehrgott. Multicriteria optimization. In *Multicriteria Optimization*, 2005.
- [6] D Fathi and JR Hoff. Shipx vessel responses (veres). *Theory manual, Marintek A/S*, 13, 2004.
- [7] Pierre Hansen. Bicriterion path problems. In Günter Fandel and Tomas Gal, editors, *Multiple Criteria Decision Making Theory and Application*, pages 109–127, Berlin, Heidelberg, 1980. Springer Berlin Heidelberg.
- [8] Charles R. Harris, K. Jarrod Millman, Stéfan J. van der Walt, Ralf Gommers, Pauli Virtanen, David Cournapeau, Eric Wieser, Julian Taylor, Sebastian Berg, Nathaniel J. Smith, Robert Kern, Matti Picus, Stephan Hoyer, Marten H. van Kerkwijk, Matthew Brett, Allan Hal-dane, Jaime Fernández del Río, Mark Wiebe, Pearu Peterson, Pierre Gérard-Marchant, Kevin Sheppard, Tyler Reddy, Warren Weckesser, Hameer Abbasi, Christoph Gohlke, and Travis E. Oliphant. Array programming with NumPy. *Nature*, 585(7825):357–362, September 2020.
- [9] Muhammad Amber Hassaan, Martin Burtscher, and Keshav Pingali. Ordered vs. unordered: a comparison of parallelism and work-efficiency in irregular algorithms. In *Proceedings of the 16th ACM Symposium on Principles and Practice of Parallel Programming, PPOPP ’11*, page 3–12, New York, NY, USA, 2011. Association for Computing Machinery.
- [10] Refael Hassin. Approximation schemes for the restricted shortest path problem. *Mathematics of Operations Research*, 17(1):36–42, 1992.
- [11] Hans Hersbach, Bill Bell, Paul Berrisford, Shoji Hirahara, Andrés Horányi, Joaquín Muñoz-Sabater, Julien Nicolas, Carole Peubey, Raluca Radu, Dinand Schepers, Adrian Simmons, Cornel Soci, Saleh Abdalla, Xavier Abellan, Gianpaolo Balsamo, Peter Bechtold, Gi-onata Biavati, Jean Bidlot, Massimo Bonavita, Giovanna De Chiara, Per Dahlgren, Dick Dee, Michail Diamantakis, Rossana Dragani, Johannes Flemming, Richard Forbes, Manuel Fuentes, Alan Geer, Leo Haim-berger, Sean Healy, Robin J. Hogan, Elías Hólm, Marta Janisková, Sarah Keeley, Patrick Laloyaux, Philippe Lopez, Cristina Lupu, Gabor Radnoti, Patricia de Rosnay, Iryna Rozum, Freja Vamborg, Sebastien Villaume, and Jean-Noël Thépaut. The era5 global reanalysis. *Quarterly Journal of the Royal Meteorological Society*, 146(730):1999–2049, 2020.
- [12] Jan Holtrop and G.G.J. Mennen. An approximate power prediction method. *International shipbuilding progress*, 29:166–170, 1982.
- [13] J. Horn, N. Nafpliotis, and D.E. Goldberg. A niched pareto genetic algorithm for multiobjective optimization. In *Proceedings of the First IEEE Conference on Evolutionary Computation. IEEE World Congress on*

- Computational Intelligence*, pages 82–87 vol.1, 1994.
- [14] Mark C. Jeffrey, Suvinay Subramanian, Cong Yan, Joel Emer, and Daniel Sanchez. A scalable architecture for ordered parallelism. In *2015 48th Annual IEEE/ACM International Symposium on Microarchitecture (MICRO)*, pages 228–241, 2015.
- [15] Lawrence Mandow and José. Luis Pérez De La Cruz. Multiobjective a\* search with consistent heuristics. *J. ACM*, 57(5), June 2008.
- [16] Ernesto Queirós Vieira Martins. On a special class of bicriterion path problems. *European Journal of Operational Research*, 17(1):85–94, 1984.
- [17] Manisha Mishra, David Sidoti, Gopi Vinod Avvari, Pujitha Mannaru, Diego Fernando Martínez Ayala, Krishna R. Pattipati, and David L. Kleinman. A context-driven framework for proactive decision support with applications. *IEEE Access*, 5:12475–12495, 2017.
- [18] Donald Nguyen, Andrew Lenharth, and Keshav Pingali. A lightweight infrastructure for graph analytics. In *Proceedings of the Twenty-Fourth ACM Symposium on Operating Systems Principles, SOSP '13*, page 456–471, New York, NY, USA, 2013. Association for Computing Machinery.
- [19] NVIDIA. Nvidia gh200 grace hopper superchip, 2023.
- [20] C.H. Papadimitriou and M. Yannakakis. On the approximability of trade-offs and optimal access of web sources. In *Proceedings 41st Annual Symposium on Foundations of Computer Science*, pages 86–92, 2000.
- [21] Keshav Pingali, Donald Nguyen, Milind Kulkarni, Martin Burtscher, M. Amber Hassaan, Rashid Kaleem, Tsung-Hsien Lee, Andrew Lenharth, Roman Manevich, Mario Méndez-Lojo, Dimitrios Proutzos, and Xin Sui. The tao of parallelism in algorithms. In *Proceedings of the 32nd ACM SIGPLAN Conference on Programming Language Design and Implementation, PLDI '11*, page 12–25, New York, NY, USA, 2011. Association for Computing Machinery.
- [22] Gilead Posluns, Yan Zhu, Guowei Zhang, and Mark C. Jeffrey. A scalable architecture for reprioritizing ordered parallelism. In *Proceedings of the 49th Annual International Symposium on Computer Architecture, ISCA '22*, page 437–453, New York, NY, USA, 2022. Association for Computing Machinery.
- [23] Anastasiia Postnikova, Nikita Koval, Giorgi Nadiradze, and Dan Alistarh. Multi-queues can be state-of-the-art priority schedulers. In *Proceedings of the 27th ACM SIGPLAN Symposium on Principles and Practice of Parallel Programming, PPoPP '22*, page 353–367, New York, NY, USA, 2022. Association for Computing Machinery.
- [24] Francisco-Javier Pulido, Lawrence Mandow, and José-Luis Pérez de-la Cruz. Dimensionality reduction in multiobjective shortest path search. *Computers & Operations Research*, 64:60–70, 2015.
- [25] Zhongqiang Ren, Richard Zhan, Sivakumar Rathinam, Maxim Likhachev, and Howie Choset. Enhanced multi-objective a\* using balanced binary search trees. *Proceedings of the International Symposium on Combinatorial Search*, 15(1):162–170, July 2022.
- [26] Oren Salzman, Ariel Felner, Carlos Hernández, Han Zhang, Shao-Hung Chan, and Sven Koenig. Heuristic-search approaches for the multi-objective shortest-path problem: Progress and research opportunities. In Edith Elkind, editor, *Proceedings of the Thirty-Second International Joint Conference on Artificial Intelligence, IJCAI-23*, pages 6759–6768. International Joint Conferences on Artificial Intelligence Organization, 8 2023. Survey Track.
- [27] Peter Sanders and Lawrence Mandow. Parallel label-setting multi-objective shortest path search. In *2013 IEEE 27th International Symposium on Parallel and Distributed Processing*, pages 215–224, 2013.
- [28] Paolo Serafini. Some considerations about computational complexity for multi objective combinatorial problems. In Johannes Jahn and Werner Krabs, editors, *Recent Advances and Historical Development of Vector Optimization*, pages 222–232, Berlin, Heidelberg, 1987. Springer Berlin Heidelberg.
- [29] Mohsin Shan and Omer Khan. Hd-cps: Hardware-assisted drift-aware concurrent priority scheduler for shared memory multicores. In *2022 IEEE International Symposium on High-Performance Computer Architecture (HPCA)*, pages 528–542, 2022.
- [30] Y.S. Shin, Vadim Belenky, W.M. Lin, K.M. Weems, A.H. Engle, K. McTaggart, Jeffrey Falzarano, B.L. Hutchison, M. Gerigk, and S. Grochowalski. Nonlinear time domain simulation technology for seakeeping and wave-load analysis for modern ship design. *Transactions - Society of Naval Architects and Marine Engineers*, 111:557–583, 01 2003.
- [31] David Sidoti, Gopi Vinod Avvari, Manisha Mishra, Lingyi Zhang, Bala Kishore Nadella, James E. Peak, James A. Hansen, and Krishna R. Pattipati. A multiobjective path-planning algorithm with time windows for asset routing in a dynamic weather-impacted environment. *IEEE Transactions on Systems, Man, and Cybernetics: Systems*, 47(12):3256–3271, 2017.
- [32] Bradley S. Stewart and Chelsea C. White. Multiobjective a\*. *J. ACM*, 38(4):775–814, October 1991.
- [33] Robert Endre Tarjan. *Data structures and network algorithms*. Society for Industrial and Applied Mathematics, USA, 1983.
- [34] George Tsaggouris and Christos Zaroliagis. Multiobjective optimization: Improved fptas for shortest paths and non-linear objectives with applications. *Theory of Computing Systems*, 45:162–186, 01 2006.
- [35] Carlos Hernández Ulloa, William Yeoh, Jorge A. Baier, Han Zhang, Luis Suazo, and Sven Koenig. A simple and fast bi-objective search algorithm. In *Proceedings of the 30th International Conference on Automated Planning and Scheduling (ICAPS)*, pages 143–151. AAAI Press, 2020.
- [36] Guido Van Rossum and Fred L. Drake. *Python 3 Reference Manual*. CreateSpace, Scotts Valley, CA, 2009.
- [37] Kai Wang, Don Fussell, and Calvin Lin. A fast work-efficient sssp algorithm for gpus. In *Proceedings of the 26th ACM SIGPLAN Symposium on Principles and Practice of Parallel Programming, PPoPP '21*, page 133–146, New York, NY, USA, 2021. Association for Computing Machinery.
- [38] Yangzihao Wang, Yuechao Pan, Andrew Davidson, Yuduo Wu, Carl Yang, Leyuan Wang, Muhammad Osama, Chenshan Yuan, Weitang Liu, Andy T. Riffel, and John D. Owens. Gunrock: Gpu graph analytics. *ACM Trans. Parallel Comput.*, 4(1), August 2017.
- [39] Arthur Warburton. Approximation of pareto optima in multiple-objective, shortest-path problems. *Oper. Res.*, 35(1):70–79, February 1987.
- [40] Yuan Yao, Zhe Peng, and Bin Xiao. Parallel hyper-heuristic algorithm for multi-objective route planning in a smart city. *IEEE Transactions on Vehicular Technology*, 67(11):10307–10318, 2018.
- [41] Guozheng Zhang, Gilead Posluns, and Mark C. Jeffrey. Multi bucket queues: Efficient concurrent priority scheduling. In *Proceedings of the 36th ACM Symposium on Parallelism in Algorithms and Architectures, SPAA '24*, page 113–124, New York, NY, USA, 2024. Association for Computing Machinery.
- [42] Lingyi Zhang, Adam Bienkowski, Matthew Macesker, Krishna R. Pattipati, David Sidoti, and James A. Hansen. Many-objective maritime path planning for dynamic and uncertain environments. In *2021 IEEE Aerospace Conference (50100)*, pages 1–10, 2021.
- [43] Yunshong Zhang, Ajay Brahmakshatriya, Xinyi Chen, Laxman Dhulipala, Shoaib Kamil, Saman Amarasinghe, and Julian Shun. Optimizing ordered graph algorithms with graphit. In *Proceedings of the 18th ACM/IEEE International Symposium on Code Generation and Optimization, CGO '20*, page 158–170, New York, NY, USA, 2020. Association for Computing Machinery.
- [44] E. Zitzler and L. Thiele. Multiobjective evolutionary algorithms: a comparative case study and the strength pareto approach. *IEEE Transactions on Evolutionary Computation*, 3(4):257–271, 1999.